Journal of Materials Chemistry B

Accepted Manuscript

ROYAL SOCIETY OF CHEMISTRY

www.rsc.org/materialsB

Graphic Abstract

A series of cationic amphiphlic copolymers (Z series) constructed from Tween 85 and low molecular weight (Mw) polyethyleneimene (LPEI) have been evaluated for the delivery of antisense 2′-O-methyl phosphorothioate RNA (2′-OMePS) both *in cell culture* and *in* dystrophic *mdx* mice. The highest efficiency of targeted exon-skipping with Z7 [T85-PEI 2k (1:1)] reaches over 8 fold, compared with 2′-OMePS only in *mdx* muscle. Which indicates that the more hydrophobic and lower PEI content within the polymer microstructure are, the greater are the 2′-OMePS delivery efficiency and exon-skipping.

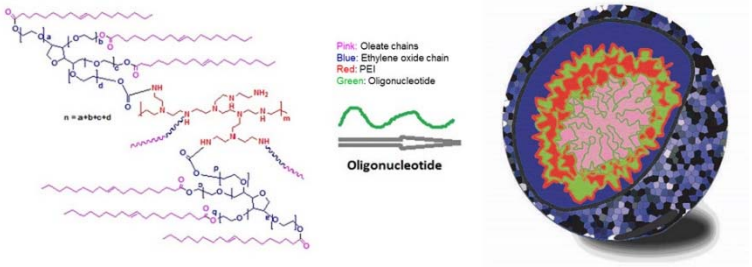

Tween 85 grafted PEIs Enhanced Delivery of Antisense 2′ -O-methyl Phosphorothioate Oligonucleotides *in vitro* and in Dystrophic *mdx* Mice

Mingxing Wang*, Bo Wu, Jason D. Tucker, Peijuan Lu, Lauren E. Bollinger, Qilong Lu*

Department of Neurology, McColl-Lockwood Laboratory for Muscular Dystrophy Research, Cannon Research Center, Carolinas Medical Center, 1000 Blythe Blvd. Charlotte, NC 28231, USA

*** Corresponding author: Mingxing Wang and Qilong Lu,** McColl-Lockwood Laboratory for Muscular Dystrophy Research, Neuromuscular/ALS Center, Carolinas Medical Center, 1000 Blythe Blvd. Charlotte, NC 28231, USA, Fax: 1-704-355-1679,

Email: mingxing.wang@carolinashealthcare.org, Phone: 1-7043555588;

Email: qi.lu@carolinashealthcare.org, Phone: 1-7043551701

Abstract

A series of cationic amphiphlic copolymers (Z series) constructed from Tween 85 and low molecular weight (Mw) polyethyleneimene (LPEI) have been evaluated for the delivery of antisense 2′-O-methyl phosphorothioate RNA (2′-OMePS) in both cell culture and dystrophic *mdx* mice. All Z copolymers improved the 2′-OMePS-induced dystrophin expression both *in vitro* and *in vivo* compared with PEI 25k formulated or 2′-OMePS alone. The most effective polymers are in the order of Z9 > Z3 > Z7, Z1, Z2, Z6 > others by formulation at the dose of 20 μg/mL in myoblast cell culture. Significantly enhanced exon-skipping of 2′-OMePS with Z polymers in *mdx* mice was obtained in the order of Z7 > Z9, Z3 > Z8, Z6 > others. The highest efficiency of targeted exon-skipping with Z7 [T85-PEI 2k (1:1)] reached over 8 folds compared with 2′-OMePS alone in *mdx* mice. Further analyses of the structure and function indicates that the more hydrophobic and lower PEI content of the polymer microstructure, the greater in delivery efficiency and exon-skipping. The unique hydrophobic interactions between the Z polymer and 2′-OMePS likely creates a more stable complex in primarily hydrophilic environments both *in vitro* and *in vivo*. The overall results suggested that Tween 85 modified LPEIs provide a promising delivery approach for applications of 2′-OMePS oligonucleotides as therapeutic reagents.

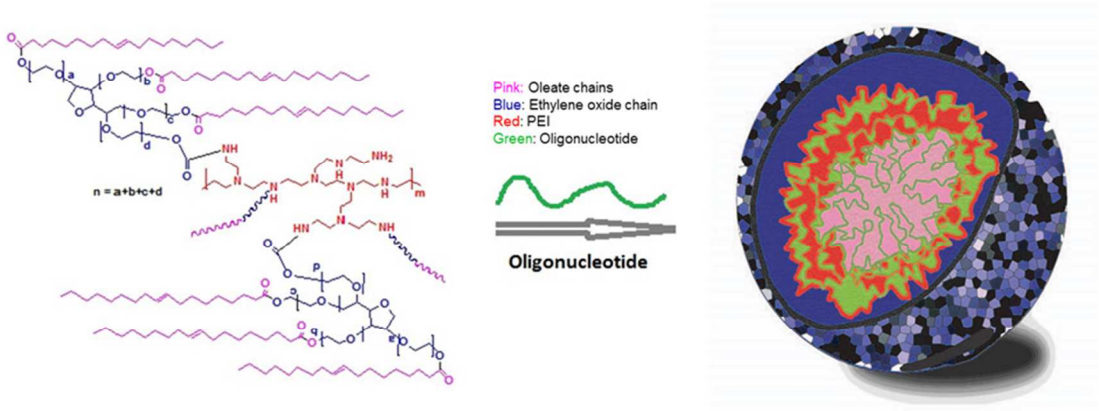

Keywords: Antisense delivery; Exon-skipping; Nanoparticle; Polyethylenimine modification; Tween 85; Muscular dystrophy

1. Introduction

Antisense oligonucleotide (AO)-mediated exon-skipping has been demonstrated as one of the most promising therapeutic strategies for the treatment of Duchenne Muscular Dystrophy (DMD), and this approach could be applicable for up to 90% of DMD patients.[1-12] DMD, an X-linked inherited muscle degenerative disorder caused by mutations in the dystrophin gene, is the most common and serious form of childhood muscle wasting disease, with an incidence of about 1 in 3500 live male births and premature lethality from respiratory or cardiac failure at around 30 years of age.[1-2] Recent trials *in vitro* and *in vivo* in *mdx* mice, canine models of DMD as well as clinical trials demonstrate that AO-mediated exon-skipping is able to induce dystrophin expression and improve muscle function. However, preliminary reports also indicate that the levels of dystrophin expression and clinical benefits of the current regime were limited, and statistical significance in preventing disease progression has not yet been convincingly obtained. This is most likely the consequence of inadequate dystrophin induction with sub-optimal dosages.[5-10] It has been well established in a number of animal models that dystrophin levels are correlated with the functional outcome of muscle, and significant therapeutic value can be achieved only with high dose AO regimes, considerably higher than the doses being used in ongoing clinical trials. However, long-term treatment with high dose could be cost-inhibitive and pose a potential risk of toxicity.[8,13,14] Among the several AO chemistries developed for exon-skipping strategy in DMD and other neuromuscular diseases, only 2′-O-methyl-phosphorothioate RNA (2′-OMePS) and phosphorodiamidate morpholino (PMO) have been tested in clinical trials. Oligomers of 2′-OMePS backbone are resistant to nuclease degradation and relatively stable in biological systems compared with natural DNA and RNA, but the presence of negatively charged phosphate groups may restrict their uptake by targeted muscle cells.[15,16] Furthermore, toxicity has limited the ceiling of dosage for clinical trials. These factors taken together suggest that an important remaining challenge is to improve delivery of AOs to targeted tissues without increasing toxicity.[17-19]

To increase delivery efficiency of negatively charged antisense oligomers like 2′-OMePS, cationic polymer-based non-viral delivery strategy has been studied. Amongst them, cationic polymethylmethacrylate (PMMA) nanoparticle loaded 2′-OMePS showed improved AOs uptake and partly restore dystrophin expression in striated muscles by weekly intrapertoneal (IP) injection.[20] The low molecular weight PEI (LPEI) constructed modifications have validated promise as antisense oligomer delivery vehicles related to their molecular size, optional hydrophilic-lipophilic balance (HLB) and low cytotoxicity, as well as their buffering capacity.[21-25] 2′-OMePS in combination with PEG550-PEI2000 copolymer enhanced exon-skipping in skeletal muscle, but the effect is limited. This is presumably due to the hydrophilic nature of the polymer hampering the interactions between the polymer with 2′-OMePS and cell and tissue membranes.[21,22] To approach this dynamic system, we have recently developed a series of amphiphilic cationic polymers, including the pluronic-PEI copolymers (PCMs), the branched poly(ester amine)s (PEAs) composed of tris[2-(acryloyloxy)ethyl]isocyanurate (TAEI) and

low molecular weight polyethylenimine (LPEI, Mw: 0.8k/1.2k/2.0k).[24,25] These polymers are effective in improving plasmid DNA (pDNA) or AO delivery *in vitro* and *in vivo* in *mdx* mice. The results indicate that delivery efficiency and cytotoxicity depend heavily on the molecular size, hydrophilic-lipophilic balance (HLB), and inclusion of cationic components, especially for the delivery of antisense-oligomer. The results also suggest that hydrophobic components of a polymer is beneficial to forming stable complexes with oligonucleotides, and to pass through the hydrophobic membrane. Given the encouraging results of our earlier studies, we report herein the study of Tween 85 (T85) modified LPEI copolymers (Zs) for negatively charged 2′-OMePS antisense oligomer *in vitro* and *in vivo* in dystrophic *mdx* mice. T85 is an amphiphilic sorbitan fatty acid ester ethoxylate, and has been reported to be able to encapsulate siRNA because of their biocompatible and chemical flexibility.[26,27] We hypothesize that T85 modified LPEI copolymers, through biodegradable carbamate linkages, could improve the oligonucleotide delivery through the beneficial properties of both components with improved cell-uptake and improved stability of polymer-oligonucleotide polyplex in circulation.[28,29] PEI can be conjugated with one to a few T85 monomers, depending on the feed ratio. It's vital for long-term clinical applications to produce polymers with defined molecular size and HLB, with high reproducibility in size and composition from batch to batch. We have previously shown that the Z polymers can significantly improve the delivery of pDNA *in vitro* and in *mdx* mice locally.[30] Our present study reveals that these Z copolymers increase 2′-OMePS induced exon-skipping efficiency significantly compared with parent LPEIs or PEI 25k formulation both *in vitro* and *in vivo*. The highest efficiency of targeted exon-skipping with 2′-OMePS AO targeted to mouse exon 23 was obtained with Z7 [T85-PEI 2k (1:1)], achieving over 8 folds increase when compared with 2′-OMePS only in the *mdx* muscle via local injection. The high efficiency and limited toxicity demonstrates the potential of the Z polymers as AO delivery vehicles.

2. Results and Discussion

2.1. Synthesis and characterization of T85-PEI copolymers (Z series)

A series of cationic amphiphlic copolymers constructed from T85 and LPEI (molecular weight 0.8k, 1.2k, 2.0k) were synthesized as previously reported (Scheme-1).[30] In short, T85 was first activated by 1, 1'-carbonyldiimidazole (CDI), then reacted with LPEI at different molar ratios . The products were purified by dialysis to remove unreacted PEI and other small molecules, followed by cation exchange chromatography to separate unconjugated excess T85. The composition of the final product was determined by ^{1}H-NMR spectra and the nitrogen content analyzed by Microanalysis. The nomenclature & characteristics of the cationic amphiphilic polymers are described in Table 1.

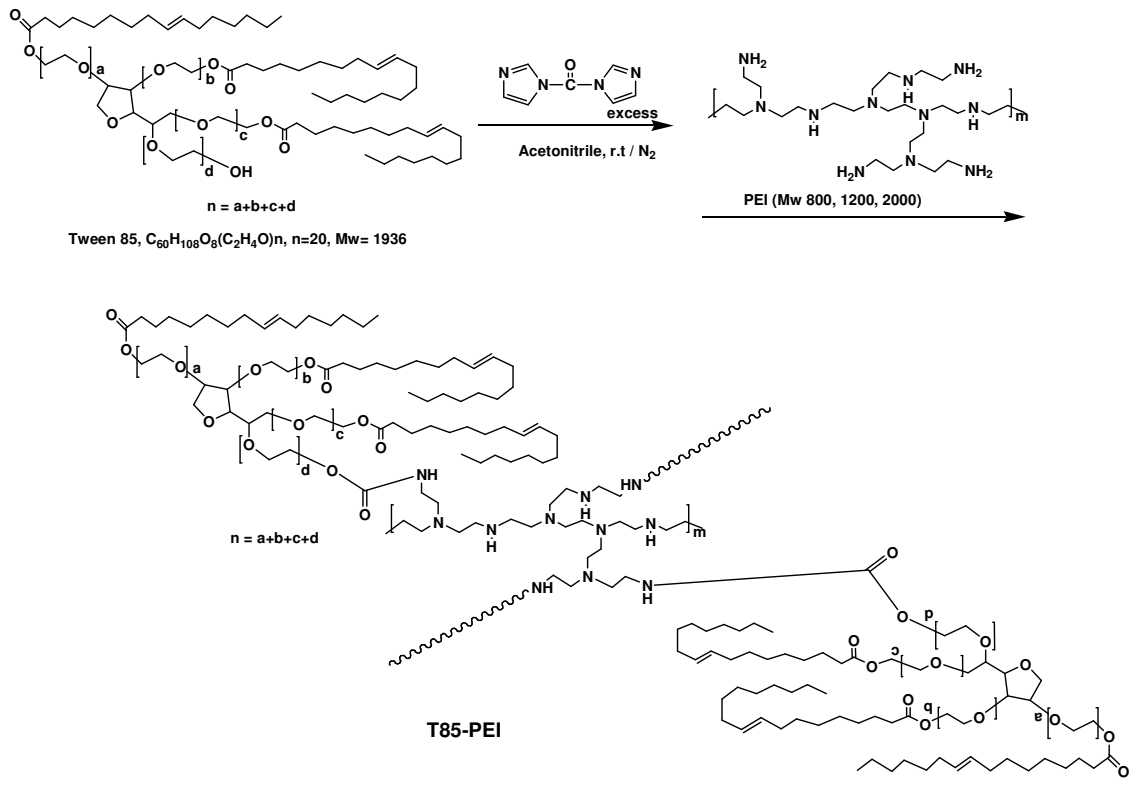

Scheme-1. Synthesis of T85-LPEI copolymers (Z polymers).

Table 1. Characteristics of T85-LPEI copolymers (Z polymers)

Code	Composition (Molar ratio) [a]	N (%) [b]	Mw(Da)		PEI (%) [d]	Grafted T85 /PEI [b]
			EA [b]	^{1}H NMR [c]		
T85	T85	0			0	
Z1	T85-PEI 0.8k (1:1)	4.43	6019.6	6981.4	13.28	6.53
Z2	T85-PEI 0.8k (1:3)	5.20	5123.5	5534.8	15.61	5.40
Z3	T85-PEI 0.8k (3:1)	4.12	6422.5	7223.6	12.46	7.02
Z4	T85-PEI 1.2k (1:1)	5.17	7766.7	8370.2	15.45	5.47
Z5	T85-PEI 1.2k (1:3)	6.24	6410.3	5796.3	18.72	4.34
Z6	T85-PEI 1.2k (3:1)	4.65	8602.2	9289.4	13.95	6.17

Z7	**T85-PEI 2.0k (1:1)**	**2.85**	**23391.8**	**25863.7**	**8.55**	**10.70**
Z8	**T85-PEI 2.0k (1:3)**	**6.97**	**9564.8**	**10808.3**	**20.91**	**3.78**
Z9	**T85-PEI 2.0k (3:1)**	**2.75**	**24242.5**	**29485.6**	**8.25**	**11.12**

a. Feed ratio of starting materials; b. Microanalysis of nitrogen; c. ^{1}H NMR analysis with 500 MHz Jeol; d. Assumed N% is 33.33 wt% in each PEI.

2.2. Polymer-oligonucleotide Polyplex Characterization

We evaluated the mixture of the Z polymers and oligonucleotides at various weight ratio (Rw) to determine the interaction between the two components using electrophoresis on agarose gel. As illustrated in **Figure 1**, all Z polymers complexed with oligonucleotides tightly at Rw = 2, and some of the polymers (Z4, Z5, Z6 and Z8) showed a high binding capacity with oligonucleotides even at Rw = 1. This lead to condensed and/or charge-neutralized complexes, as indicated by the shifting of the bands stained with ethidium bromide towards significantly higher molecular size. These results are consistent with the expectation that negatively charged oligonucleotides are progressively neutralized by the increasing amount of positive charged Z polymers as the ratio of polymer/oligonucleotide increased. The slightly weak binding of Z1-Z3, Z7 or Z9 to the oligonucleotide is likely due to the higher molecular weight with lower PEI content compared to the other Zs within their corresponding subseries. The results also disclosed that the binding affinity of the Zs to short oligonucleotides is stronger than that to large pDNA under the same conditions, suggesting that the polymers condense smaller oligomers more effectively.[21,30] The results demonstrate that polymer size, cationic and lipophilic components in a polymer are critical for the effective condensation between the polymer carrier and delivery cargo, and further affect delivery performance. However, it is unlikely that electrostatic interaction is the only mechanism by which amphiphilic T85 modified PEIs form complexes with negative charged oligonucleotides.

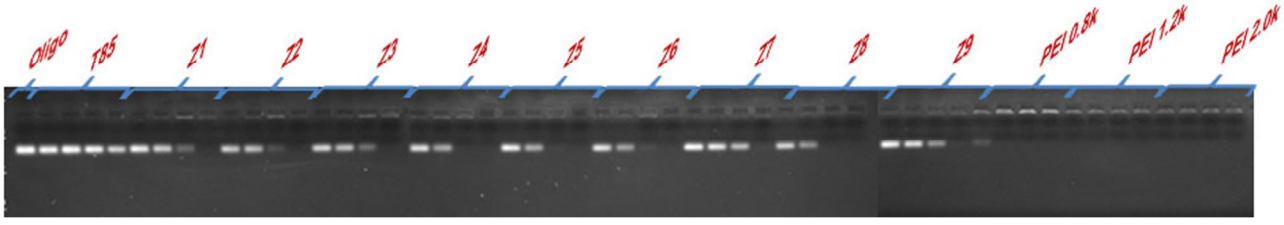

Figure 1. Electrophoretic mobility of polymer/oligonucleotide complexes at four weight ratio of Rw = 0.2 , 0.5 , 1 and 2 (from left to right for each polymer). 1 µg oligonucleotide in a total of 24 µL medium was used. The 1st lane on the left is loaded with 1 µg oligonucleotide only.

The particle size of cargo-polymer complex is important for effective gene transfection, and low-end nano-sized particles are generally considered preferable. We therefore examined the complex of Z polymers and oligonucleotides (ZO-complex) by Dynamic Light Scattering (DLS). As expected, all of the modified polymers condensed oligonucleotides into particles below 500 nm, and the average surface charges of the polyplexes ranged from -15.5 to 7.5 mV under the tested ratios from Rw = 1 to Rw =10. A homogenous hydrodynamic diameter (D_H) below 200 nm, with a narrow size distribution (PDI < 0.3), was observed at the Rw of 5 (**Figure 2A**). To gain further insight into the ZO-complexes, we performed Transmission Electron Microscopy (TEM) analysis that demonstrated the nanoparticles were well defined, spherical, and uniformly distributed with sizes between 30-50 nm at a representative Rw = 5. In contrast, the polymer alone showed homogeneous particles smaller than the ZO-complexes, likely the consequence of a self-assembling ability of its amphiphilic nature. Oligonucleotide alone formed heterogeneous particles due to aggregation (**Figure 2B**).[31] The smaller particle size observed under TEM in comparison with that from DLS analysis was due to the TEM processing which dries the samples causing shrink in particle size.[25,30] These results therefore suggest that the T85 components in the Z polymers were able to form particles favorable for delivery by preventing PEI from aggregation with oligonucleotides.

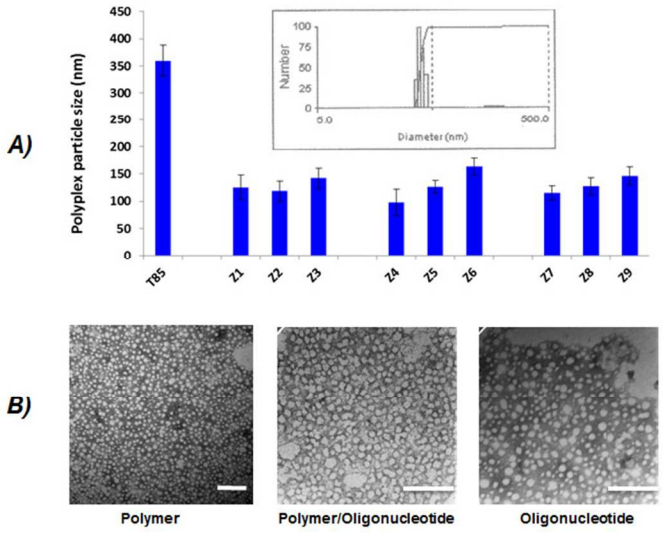

Figure 2. Biophysical properties of polymer-oligonucleotide complex (Rw = 5). A) Particle sizes analyzed by DLS, Inserted is the distribution of size; B) Negative staining TEM images (scale bar 200 nm).

2.3. Stability of Z polymer-oligonucleotide Polyplexes in the Presence of Serum and Heparin

Serum, which contains numerous negatively charged molecules from proteins to glycosaminoglycans (GAG), has a significant effect on gene transfection efficiency *in vitro* and *in vivo*, especially when positively charged vectors are used as delivery carriers. Anionic serum components can compete with negatively charged oligonucleotides

for the binding of positively charged polymers, leading to the dissociation of the oligonucleotide from the carrier and variable modulation of gene delivery effects. The presence of DNAase in the serum and interstitium can degrade accessible oligonucleotides thus reducing the effective concentration. The stability of the oligonucleotide-polymer complex in the presence of serum is therefore an important factor to be considered for both *in vitro* and *in vivo* applications of gene carriers. To determine the stability of ZO- complex, we prepared them at fixed ratios and added FBS to a final concentration of 0, 10, 25, and 50%, followed by analysis of the mixtures with gel electrophoresis (**Figure 3A**). The serum components react with oligonucleotides to form complexes indicated by an increase in the size of the oligomer bands with increasing amounts of FBS, or to compete with positively charged polymers, leading to the dissociation of oligonucleotide from complexes. Serum had no apparent influence on the ZO-complexes formed at Rw = 2. This is similar to the complexes of oligonucleotide formulated with PEI. However, some dissociation of oligonucleotide was observed with increasing FBS from ZO-complexes based on Z7 and Z9 polymers, which contain lower PEI content compared to other Z polymers. This result suggests that LPEIs within the cationic amphiphilic polymers still maintain their binding affinity and strength, thereby preventing the bound oligonucleotides from being replaced by serum components.

Heparin is a highly sulfated glycosaminoglycan (GAG) with a linear polysaccharide structure and a strong negative charge. Heparin is the major components in the extracellular matrix of many tissues, and can also be found inside cells and on cell surface.[32] We therefore evaluated the binding strength of polymer- oligonucleotide complex in the presence of heparin. When the ZO-complexes at Rw = 2 was incubated with saline solution containing 10 µg/mL sodium heparin, EB signals for oligonucleotide remained in the loading well in all polymer samples except for Z7 and Z9. Increasing the concentration of sodium heparin to 25 µg/mL led to near complete dissociation of the oligomer from the complexes of Z1, Z2, Z3, Z4, Z7 and Z9 formulation. However, the majority of oligonucleotide within Z5, Z6 and Z8 formulated complexes remained polymer-bounded. These three polymers contained higher PEI composition and/or higher Mw compared with the rest Z polymers. All oligonucleotide was dissociated from the ZO-complexes when the concentration of sodium heparin increased to 50 µg/mL except for Z8, which has a high Mw (9,564.8) and the highest PEI content (20.91%). Complexes of PEI and oligonucleotide remained intact in the presence of sodium heparin, even at 50 µg/mL (**Figure 3B**). These results further suggest that the increasing binding affinity of Z polymers to oligonucleotides is associated with increasing % of PEI and Mw of Z polymers as well as the flexibility of T85 within the polymers. Since concentration of heparin varies greatly in different tissues, concentration-dependent release of the oligonucleotide from ZO-complexes in the presence of heparin could be utilized in advancing vector design for controlled release of cargos with tissue specificity.

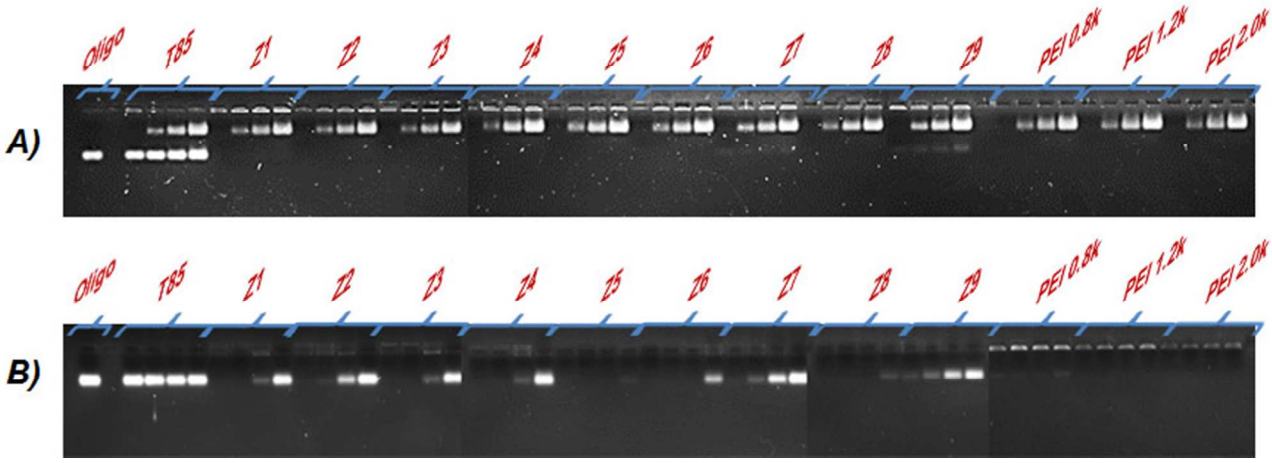

Figure 3. Stability of complexes [Polymer/oligonucleotide = 2/1(Rw = 2)] to serum or heparin. A) In the presence of serum. 4 lanes for each polymer with FBS concentration of 0, 10, 25, 50% from left to right; The middle bands between the oligonucleotide (bottom bands) and wells (top bands) are non-specific binding of EB to serum components. B) In the presence of sodium heparin (0, 10, 25, 50 µg/mL) from left to right.

2.4. Evaluation of 2′-OMePS delivery in C2C12 myoblast cell lines expressing GFP/hDysE50

The cytotoxicity of polymers in C2C12E50 cells was evaluated by [3-(4,5-dimethylthiazol-2-yl)-5-(3-carboxymethoxyphenyl)-2-(4-sulfophenyl)-2H-tetrazolium] (MTS)-based assay. PEI 2k kept very high cell viability, approximately 73%, at a dose of 20 µg/mL. In contrast, high Mw PEI 25k displayed much higher cell toxicity with cell survival at 60%, 45% and 25% at a dose of 4 µg/mL, 10 µg/mL and 20 µg/mL, respectively. The Lipofectamine-2000 (LF-2k) showed slightly lower toxicity than PEI 25k at the same doses. All Z polymers at a dose of 20 µg/mL showed cell survival of over 75%, expect Z8 which displayed relatively higher toxicity (67% live cells). This likely resulted from the higher PEI composition (**Figure 4**). The cytotoxicity data suggests that the toxicity of the T85 modified LPEI does not increase as increasing polymer size. We reason this is due to the substitution of the primary and/or secondary amines of PEI with the biocompatible T85.[26] We further examined the effect of Z polymers at 4 different dosages (4, 10, 20, and 40 µg/mL) with 2′-OMePS on exon-skipping in the C2C12E50 cell line. The 2′-OMePSE50 sequence (5′ – AACUUCCUCUUUAACAGAAAAGCAUAC – 3′) targeting the inserted human dystrophin exon 50 within the GFP coding region was used. The cells were treated with the 2′-OMePSE50 at a fixed amount (4 µg/mL) formulated with each Z polymer. Transfection efficiency (TE) of formulated 2′-OMePSE50 was determined by fluorescence microscopy analysis two days after transfection. The results exhibited that all Z polymers at the dose of 10 µg/mL produced enhanced GFP expression as compared to the 2′-OMePSE50 alone. The highest levels of GFP expression were achieved at the dose of 20 µg/mL with most Z polymers. No apparent GFP enhancement

was further observed when the dose of Z polymers increased up to 40 µg/mL, probably due to the aggregation of polymer-AO complex under the high dose ratio (Rw = 10). As illustrated in **Figure 5**, Z7 mediated 2′-OMePSE50 delivery indicated dose-dependent GFP expression, representing the oligonucleotide-induced exon-skipping and the restoration of the GFP reading frame. The delivery efficiency and toxicity of Z polymers (at the dose of 10 and 20 µg/mL) formulated 2′-OMePS (4 µg/mL) was studied therefore quantitatively by fluorescence microscopy and FACS (**Figure 6**). The efficiencies of exon-skipping of 2′-OMePS with the Z polymers were clearly higher than that of T85 mediated or naked 2′-OMePS, reaching over 75% with Z1, Z2, Z3, Z4, Z6, Z7, Z9 at the dose of 20 µg/mL, and with Z5, Z6, Z7, Z8 at the dose of up to 10 µg/mL. In contrast, 2'-OMePS alone and in combination with T85, PEI 25k and LF-2k exhibited 4%, 33%, 45%, and 1.5% at the optimal concentration, respectively. Clearly, the results indicate that a combination of amphiphlic and cationic ingredients together are preferred as delivery carrier for enhancing delivery efficiency of 2′-OMePS. Cytotoxicity of the ZO-complexes was dramatically lower than that of PEI 25k or LF-2k formulated oligonucleotide complexes. This is in agreement with the comparison between Z polymers and control polymers alone in cell culture system.

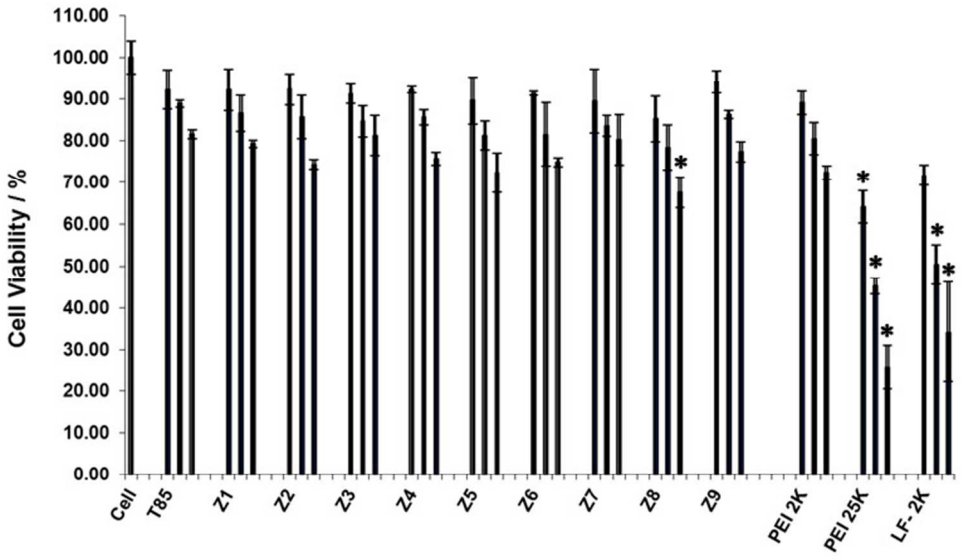

Figure 4. The cytotoxicity of the Z polymers in C2C12E50 cell lines with MTS-based cell viability assay. The polymer dosages are 4, 10, 20 µg/mL from left to right for each sample. Cells were seeded in 96 well plates at an initial density of 1 x 10^4 cells/well in 0.2 ml growth media. The results are presented as the mean ± SD in triplicate (Student's t-test, *$p \leq 0.05$ compared with untreated cell as a control).

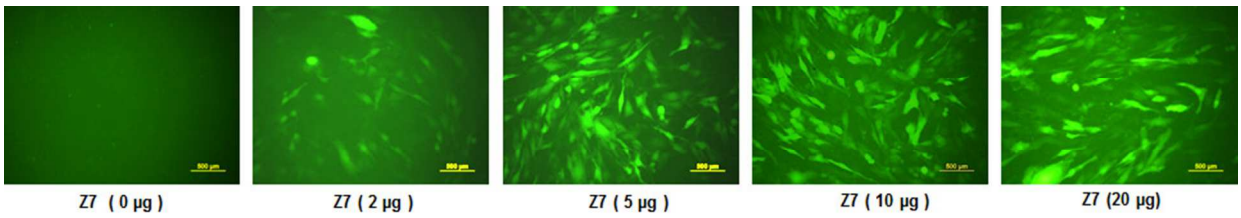

Figure 5. Dose-dependent GFP expression of polymer Z7 formulated 2′-OMePS: 2 μg 2′-OMePS with polymers in 0.5 mL 10% FBS-DMEM incubated under 37°C, 10% CO_2 environment. The images were taken 48 hrs after transfection.

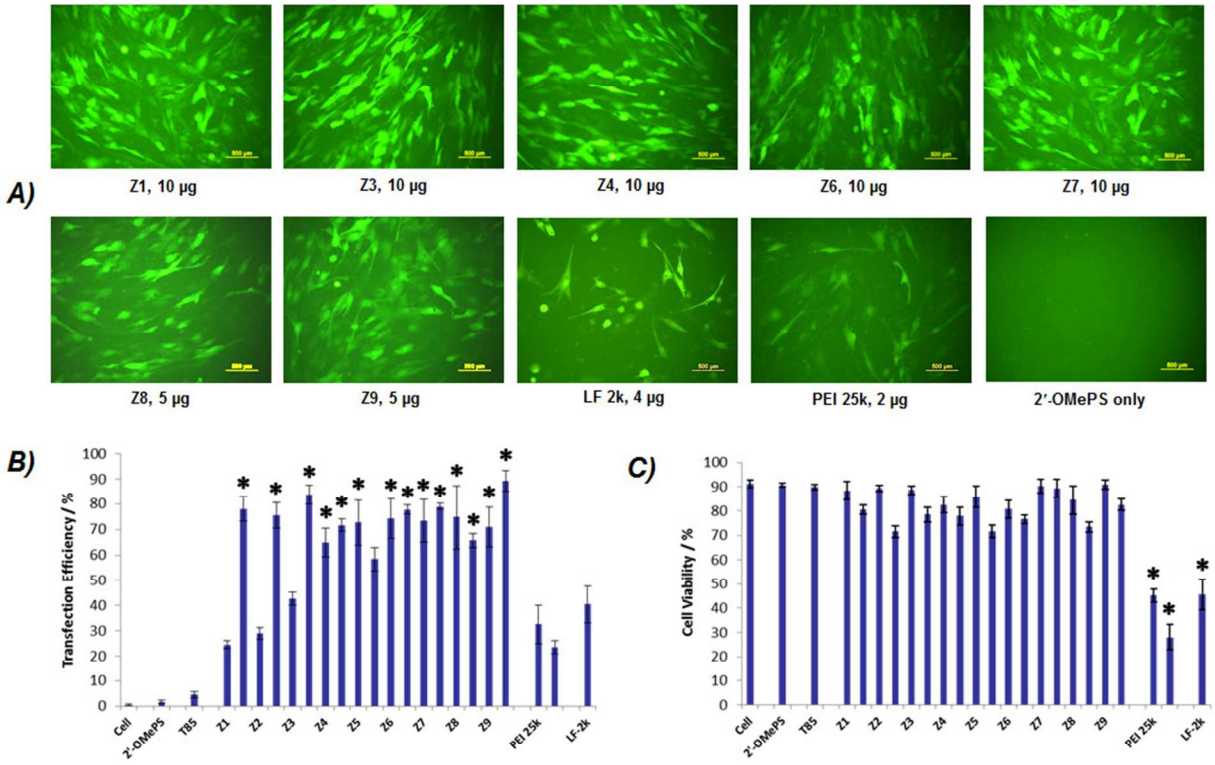

Figure 6. A) Representative fluorescence images of 2′-OMePSE50 -induced exon-skipping in C2C12E50 cell line. The images were taken 48hr after treatment. Original magnification, x100. B) Transfection efficiency of 2′-OMePSE50 formulated with polymers (Student's t-test, $*p \leq 0.05$ compared with 2′-OMePS only). C) Cell viability (Student's t-test, $*p \leq 0.05$ compared with untreated cells as a control). 2 μg of 2′-OMePSE50 were formulated with Zs (5,10 μg), and PEI-25k (2, 5 μg), LF-2k (4 μg) formulated as controls in 0.5 mL 10% FBS-DMEM medium, respectively. The results are presented as the mean ± SD in triplicate.

To further characterize cellular uptake of ZO-complexes, the FLTC-labeled Z9 was complexed with Cy3-labeled oligonucleotide (Cy3-Oligo) at weight ratio of 5:1 and examined by confocal microscopy (**Figure 7**). Without Z polymer, oligonucleotide alone showed very weak diffused signal within the target cells. In contrast, fluorescent signals with the ZO-complex were much stronger. Signals are predominantly cytoplasmic and perinuclear. While the two signals for Z9 polymer and oligonucleotide were generally co-distributed indicated by yellow on the merged image (D), punctuate signal (small dots) were only observed in green in cytoplasm. Although the precise localization of the signals remains to be determined, the pattern suggests the two components of the complexes underwent a certain degree of differential transportation after entering cytoplasm. The enhanced uptake for the ZO-complexes is likely due to strong and stable interaction between polymer and oligonucleotide in complex as demonstrated by DLS and TEM analyses.

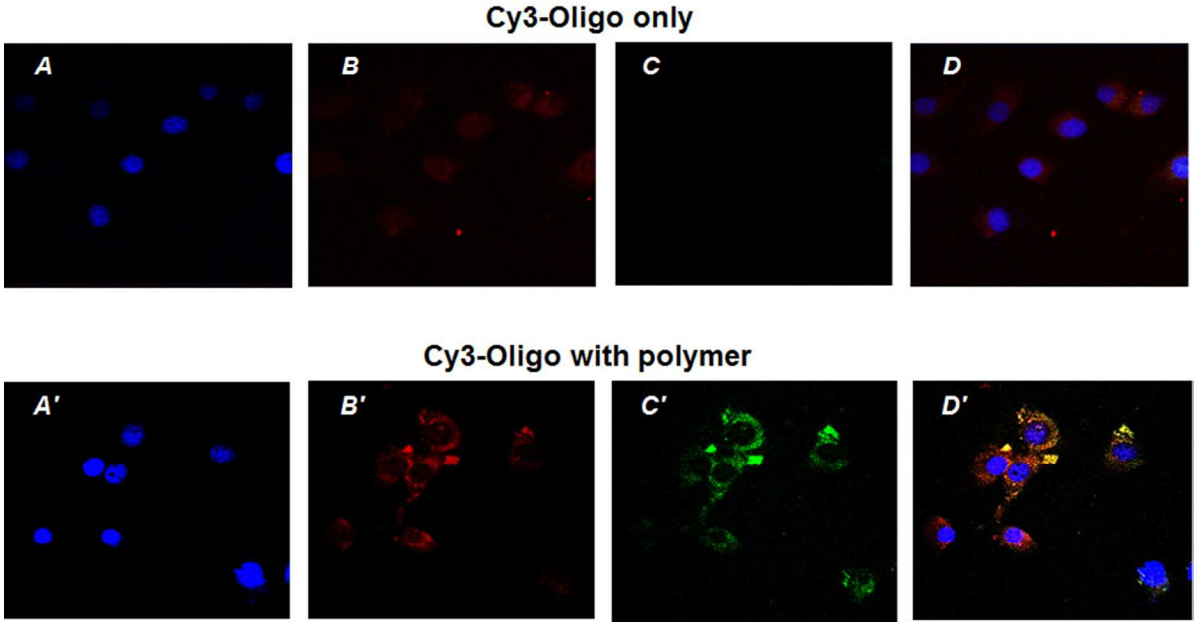

Figure 7. Intracellular interaction of FITC-labeled-Z9 formulated with Cy3-labeled-oligonucleotide (Cy3-Oligo) in C2C12 fibroblast cell line (10 µg polymer in 0.5 mL 10% FBS-DMEM with Cy3-Oligo 2 µg). (A-A′) Nuclei were stained with Hoechst 33258 (blue fluorescence); (B-B′) Red fluorescent signal from labeled Cy3-Oligo; (C-C′) Green fluorescence arising from FITC-labeled-polymer; (D-D′) Merged image (A+B+C) demonstrating localization of the polymer relative to AO signal. Yellow fluorescence on the merged image (D) indicates where FITC-polymer and Cy3-Oligo are collocated, contrasted with red signal from oligonucleotide dissociated from the initial polymer-AO complex. 40 x magnification.

2.5. Delivery of 2'-OMePS with Zs *in vivo*

We evaluated the effects of the Z polymers on 2′-OMePS delivery *in vivo* by intramuscular (i.m.) injection to the TA muscles of *mdx* mice aged 4-5 weeks with the 2′-OMePSE23 targeting mouse dystrophin exon 23. The *mdx* mouse contains a nonsense mutation in exon 23 and lacks the functional dystrophin protein. Targeted removal of the mutated exon 23 is able to restore the reading-frame of dystrophin transcripts and thus the expression of dystrophin protein. All Z polymers were examined at the dose of 10 μg mixed with 5 μg of 2′-OMePSE23 in 40 μL saline for injection. Treated TA muscles were harvested 2 weeks following injection. Immunohistochemistry showed that 2′-OMePSE23 alone induced below 3% dystrophin-positive fibers in cross-section of the treated muscles. The numbers of dystrophin-positive fibers increased up to 2.5 - 8 folds in the muscles treated with 10 μg Z polymers formulated 2′-OMePSE23. In particular, dystrophin-positive fibers were induced to 13%, 18%, 16%, 24%, 16% and 19% in the muscles treated with Z1, Z3, Z6, Z7, Z8 and Z9 formulated 2′-OMePSE23, respectively. In contrast, T85-mediated 2′-OMePS delivery produced around 5% positive fibers (**Figure 8**). The levels of exon-skipping measured by RT-PCR were 60.2%, 23.4%, 21%, 34.5%, 57%, 65.3%, and 23% for Z1, Z3, Z6, Z7, Z8, Z9 and 2′ -OMePS only, respectively. Western-blot showed dystrophin protein levels at 51.2%, 50.8%, 57.6%, 42.7%, 46.6%, 46.5% for Z1, Z3, Z6, Z7, Z8, Z9 mediated 2′ -OMePS delivery, respectively compared with C57 normalized as 100%. Quantitative *in vivo* data demonstrates that the more T85 component (more lipophilic and lower cationic charge) within the polymer, the higher the efficiency as a 2′-OMePS delivery carrier. Hematoxylin and Eosin (H&E) staining revealed no signs of increased inflammation, tissue remodeling, or fiber necrosis compared with untreated *mdx* muscle. This is consistent with our previous results that the T85 modified LPEI polymers were of limited cytotoxicity *in vitro* and *in vivo*.[30]

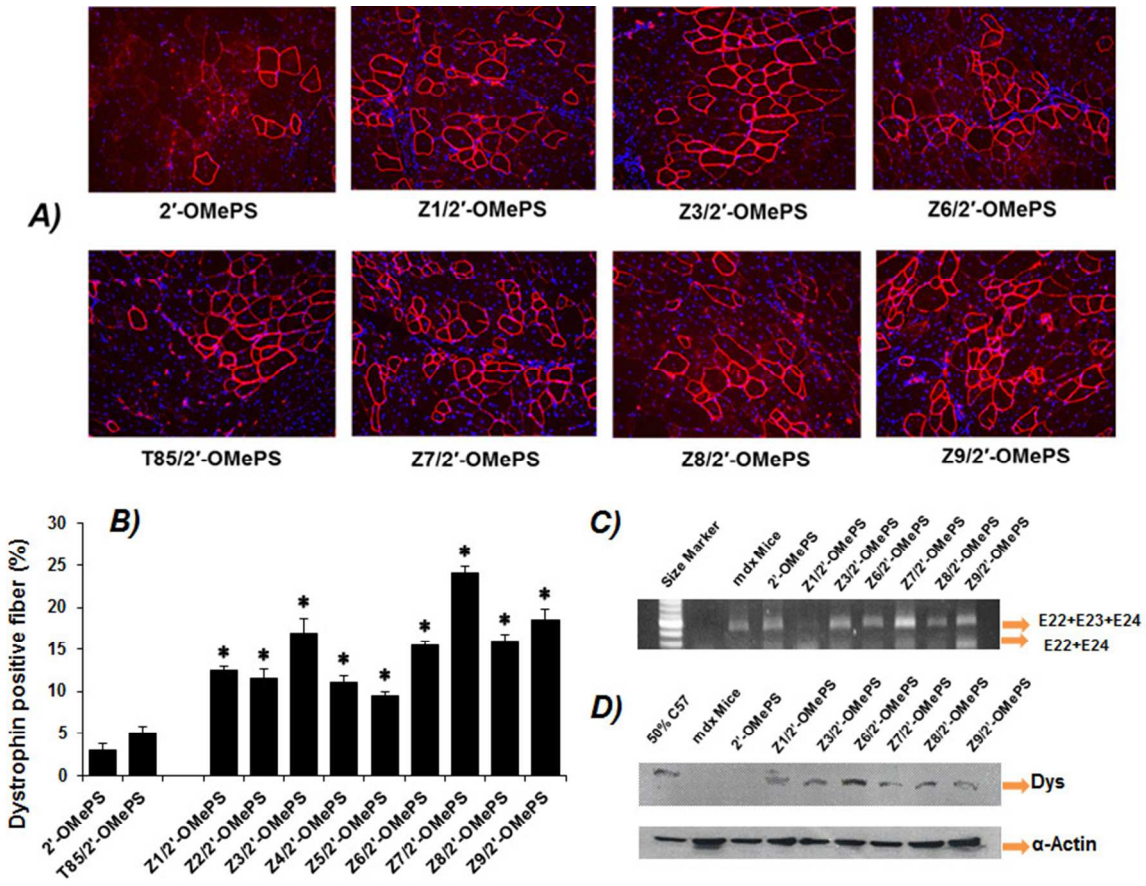

Figure 8. Dystrophin exon-skipping and protein expression following i.m. administration of 2′-OMePS E23 without and with polymers in TA muscle of *mdx* mice (aged 4-5 weeks) after 2 week treatment. Muscles were treated with 2′-OMePSE23 (5 µg) and polymer (10 µg) in 40 µL saline. 2′-OMePS E23 (5 µg) only was used as control: ***A)*** Restoration of dystrophin in TA muscle was detected by immunohistochemistry with rabbit polyclonal antibody P7 against dystrophin. Blue nuclear staining with DAPI (4,6-diamidino-2-phenylindole). Original magnification, x100. ***B)*** The percentage of dystrophin-positive fibers in a single cross-section induced by 2′-OMePS E23 with/without polymer formulation (average ± SD, n = 5, Student's t-test, $*p \leq 0.05$ compared with 5 µg 2′-OMePSE23). ***C)*** Detection of exon 23 skipping by RT-PCR. Total RNA (100 ng) of from each sample was used for amplification of dystrophin mRNA from exon 20 to exon 26. The upper bands (indicated by E22+E23+E24) correspond to the normal mRNA and the lower bands (indicated by E22+E24) correspond to the mRNA with exon E23 skipped. ***D)*** Western blot demonstrates the expression of dystrophin protein from treated *mdx* mice compared with C57BL/6 and untreated *mdx* mice. Dys: dystrophin detected with a monoclonal antibody ManDys 1. a-Actin was used as the loading control.

3. Conclusions

The study of T85 modified LPEI copolymers for 2′-OMePS delivery *in vitro* and *in vivo* of dystrophic *mdx* mice revealed that delivery efficiency and toxicity depends on the molecular size, composition and hydrophobic-lipophilic balance (HLB) of the polymers. Improved exon-skipping efficiency by formulation was observed *in vitro* with all modified polymers compared with PEI 25k or LF-2k, and the degree of efficiency was found in the order of Z9 > Z3 > Z7, Z1, Z2, Z6 > others at the dose of 20 μg/mL. The *in vivo* study in *mdx* mice demonstrated significantly enhanced exon-skipping of 2′-OMePS with low toxicity with the Z polymers in the order of Z7 > Z9, Z3 > Z8, Z6 > others. However, further optimization of individual Z polymer is needed for achieving maximal delivery effect with least toxicity to specific application. Delivery performance depends on both the hydrophobic and electrostatic interaction between the polymer and short, single-stranded 2′-OMePS oligonucleotides. The results indicate the importance of PEG and lipid components in cationic polymers for effective oligonucleotide delivery, and support the view that endogenous, lipid modified PEI were more effective to encapsulate siRNA when compared with parent PEI. [27] The unique hydrophobic interaction between the Z polymer and 2′-OMePS creates a more stable complex in primarily hydrophilic environments and further enhances complex-plasma membrane interactions both *in vitro* and *in vivo*. The superior ability to condense and deliver oligonucleotides with these Z polymers is likely to be related to the chemical structure of the amphiphilic T85 and appropriate positive charges of polymer/oligonucleotide complex. Therefore, it was not surprising to find Z7, Z9 and Z3 showing a better transfection performance for 2′-OMePS delivery both *in vitro* and *in vivo*, particularly the Z7 which was the best among the Z polymers *in vivo*. The variability of individual Z polymers for delivery of negatively charged 2′-OMePS and pDNA highlights the complexity of the interaction between polymer and their delivery cargos, the difference in the delivery mechanism, and the difficulty in achieving optimization with high efficiency and low toxicity. The flexibility of the Z series polymers as delivery vectors for both large size pDNA and small oligonucleotides *in vitro* and *in vivo*, shows their potential of a broad spectrum of therapeutic applications.

4. Experimental Section

4.1. Materials

A series of cationic amphiphlic copolymers constructed from Tween 85 and low molecular weight (Mw) polyethyleneimene (LPEI) were synthesized as previous reported.[30] Cell culture media Dulbecco's Modified Eagle's Medium (DMEM), fetal bovine serum, L-glutamine and HEPES buffer solution (1M), penicillin-streptomycin, and 3-(4,5-dimethylthiazol-2-yl)-5-(3-carboxymethoxyphenyl)-2-(4-sulfophenyl)-2H-tetrazolium (MTS) were purchased from GIBCO, Invitrogen Corp (NY, USA). An arbitrary single-stranded 20-mer deoxyoligonucleotide was used as a model antisense oligonucleotide (AO), with the sequence 5′-

GGCCAAACCTCGGCTTACCT-3′ (phosphodiester), for the physicochemical study of polymer-oligonucleotide polyplex. AOs modified by 2′-O-methylation and phosphorthioation 2′-OMePSE50 (5' – AACUUCCUCUUUAACAGAAAAGCAUAC – 3′) targeting human dystrophin gene exon 50, 2′-OMePSE23 (5'-GGCCAAACCUCGGCUUACCU-3′) targeting mouse dystrophin gene exon 23, Cy3-Oligonucleotide (5′-GGCCAAACCUCGGCUUACCU-3′) used for delivery *in vitro* and *in vivo* were purchased from GenScript (NJ, USA). All other chemicals were purchased from Sigma-Aldrich (MO, USA), unless otherwise stated.

4.2. Complexation study of polymer/oligomer

Agarose gel electrophoresis: All polymer-oligonucleotide complexes were freshly prepared before use with different polymer/oligonucleotide weight ratios (Rw) by vortex of oligonucleotide and polymer stock solutions. The complexes were incubated at room temperature for 30 minutes in 24 µL volume and loaded on 1% agarose gel with ethidium bromide (EB, 0.1 µg/mL) included into the gel to visualize the localization of the oligonucleotide. Electrophoresis was carried out with tris-acetate (TAE) buffer at 100 V for 40 minutes and analyzed on UV illuminator.

Resistance to Serum and Heparin: To determine the stability of the polymer-oligonucleotide complexes in the presence of polyanions, such as serum or heparin, 20 µL polymer-oligonucleotide complexes of Rw = 5 were added to 0.5 mL Eppendorf tubes. Fetal Bovine Serum (FBS) was then added by volume to achieve final concentrations up to 50%, mixed, and incubated for 30 minutes at 37 ^{o}C. These samples were then electrophoresed in 1% agarose gel to determine the stability of the complexes. For the analysis of their resistance to heparin, varying amounts of 1µg/µL heparin sodium were added to polymer-oligonucleotide complexes to achieve final concentrations of 0, 10, 25, 50 µg/mL. Samples were then incubated at 37 ^{o}C for 30 minutes and electrophoresed.

Particle size, zeta potential determination by Dynamic Light Scattering (DLS): The hydrodynamic diameters (D_H) of polymer-oligonucloetide polyplexes in 0.9% sodium chloride were determined by DLS at a 90 ^{o} measurement angle with Zetaplu Zeta Potential Analyzer 90 Plus/BI-MAS (Brookhaven Instrument Co. USA) equipped with a 15 mV solid-state laser operated at a wavelength of 635 nm. Briefly, 1 mL of polyplex solution containing 5 µg of oligonucleotide was prepared at various Rws (1 to10) and incubated 30 minutes at 4 ^{o}C, then the polyplex size was measured by photon correlation spectroscopy. For data analysis, the refractive index (1.33) and viscosity (0.89) of water at 25 ^{o}C were used. Polystyrene nanospheres were used to check the performance of the instrument.

The zeta potential (surface charge) of polyplex was determined at 25 ^{o}C using the same apparatus equipped with a 658 nm laser. Above samples were diluted to 10 times with de-ionized water to ensure the measurement operated under low ionic strength, where the charge of particles can be measured accurately.

Morphology analysis: The polymer-oligonucleotide polyplex (Rw = 5) solution containing 1 µg of oligonucleotide was prepared in 200 µL 0.9% NaCl, pH 7.4 medium, and corresponding polymer and oligonucleotide only as a comparison. The solutions were analyzed using Transmission Electron Microscopy (TEM, Phillips CM-10, Philips Electronic North America Corp., Andover, MA, USA). Samples were prepared using negative staining with 1% phosphotungstic acid. Briefly, one drop of sample solution was placed on a formvar and carbon coated grid (Electron Microscopy Sciences, Hatfield, PA) for 1 hour, and the grid was blotted dry, followed by staining for 3 minutes. The grids were, once again, blotted dry. Samples were analyzed at 60 kV. Digital images were captured with a digital camera system from the 4 pi Analysis (Durham, NC, USA).

4.3. In vitro study

Cell viability: Cytotoxicity was evaluated in C2C12E50 cell line using the MTS-based assay. Cells were seeded in a 96-well tissue culture plate at 1 x 10^4 cells per well in 200 µL 10% FBS-DMEM. Cells achieving 70-80% confluence were exposed to polymer at different doses for 24 hours, followed by the addition of 20 µL of Cell Titer 96®Aqueous One Solution Proliferation Kit (Promega Corporation, Madison, MI, USA). After further incubation for 4 hours, the absorbance was measured at 570 nm using Tecan Infinite F500 Plate reader (Tecan US, Inc, Morrisville, NC, USA) to obtain the metabolic activity of the cell. Untreated cells were taken as controls with 100% viability and wells without cells as blanks, the relative cell viability was calculated by: $(\boldsymbol{A}_{\text{treated}}\text{-}\boldsymbol{A}_{\text{background}})$ x $100/(\boldsymbol{A}_{\text{control}}\text{-}\boldsymbol{A}_{\text{background}})$. All viability assays were carried out in triplicate.

In vitro transfection: The C2C12 E50 cell has a human dystrophin exon 50 sequence (hDysE50) placed inside the coding sequence of GFP gene under control of an actin promoter. Upon the effect of antisense oligonucleotide targeting exon hDysE50, the hDysE50 sequence is spliced out and the GFP coding sequence rejoined back in-frame.

C2C12 or C2C12E50 cells were cultured in 10% FBS-DMEM and kept in a 10% CO_2 humidified incubator at 37 ^{o}C. Approximately 5 x 10^4 cells per well were seeded in a 24 well plate in 500 µL medium and allowed to reach 70-80% confluence prior to transfection experiments. Cell culture medium was replaced before the addition of polymer/2′-OMePSE50 cargos formulated with varying Rw. PEI 25k was used as positive control for delivery. Transfection efficiency was visualized using an Olympus IX71 fluorescent microscope (Olympus America Inc., Milville, NY, USA). Digital images were taken using the Olympus DP Controller and DP Manager software (Olympus America Inc., Milville, NY, USA). Transfection efficiency was also examined using flow cytometry to

quantitatively gauge the GFP expression level. Cells were washed with PBS (1X) and released from the culture vessel with 0.05% Trypsin-EDTA, neutralized by FBS, pelleted by centrifugation and then re-suspended in 1 mL PBS. Samples were run on a FACS Calibur flow cytometer (BD, Franklin Lakes, NJ, USA). Minimum 1 x 10^4 cells were counted and analyzed with CellQuest Pro (BD, Franklin Lakes, NJ, USA) software package.

Fluorescence labeling of polymers: The polymer was labeled with Fluorescein isothiocyanate (FITC) as described in a previous study with some modification.[22] The over excess FITC, dissolved in DMSO, was added drop-wise to polymer in PBS (pH 7.4) solution. The solution was then incubated at room temperature with continuous stirring in the dark overnight. The labeled polymer was dialyzed with MWCO 2000 membrane against PBS (pH 7.4) for 24 hours and then distilled water for 12 hours. The product was finally lyophilized and kept at -20 ^{o}C.

Cellular uptake and intracellular localization: For cellular uptake and intracellular localization study, Cy3-labeled oligonucleotide was combined with FITC-labeled polymer at a predetermined ratio, followed by imaging under confocal microscopy. C2C12 cells were seeded onto 8 well glass Lab-Tek II® chamber slides (Scientific, Ocala, FL, USA) at 5 x 10^3 cells/well, and cultured to 70% confluence before the addition of polymer-oligonucleotide formulation for testing. 24 hours after addition of the samples the cells were washed with warm PBS (0.1M, pH 7.4) to remove any residual polymer-oligonucleotide complex not taken up by cells. Cells were then counterstained with Hoechst 33258 (Life Technologies, Carlsbad, CA, USA) for 20 min at 37 ^{o}C. Subsequently, the cells were washed with PBS three times and then incubated with 200 µL PBS. The cells were examined using Zeiss LSM-710 inverted confocal microscope (Carl Zeiss Microscopy, LLC; Thornwood, NY, USA), and the resulting images were analyzed for uptake and localization by single channel images. Colocalization of polymer/oligonucleotide to the lysosome was visualized by merging channel images.

4.4. In vivo delivery and antibodies, immunohistochemistry

This study was carried out in strict accordance with the recommendations in Guide for the Care and Use of Laboratory Animals of the National Institutes of Health. The protocols were approved by the Institutional Animal Care and Use Committee (IACUC), Carolinas Medical Center (Breeding protocol: 10-13-07A; Experimental protocol: 10-13-08A). All injections were performed under isoflurane anesthesia, and all efforts were made to minimize suffering.

Animals and intramuscular (i.m.) injections: Dystrophic *mdx* mice aged 4-5 weeks were used for *in vivo* testing (5 mice each in the test and control groups) unless otherwise stated. Four muscles were examined for each experimental group.

The 2′-OMePSE23 (+02-18) (5′-GGCCAAACCUCGGCUUACCU-3′) targeting the boundary sequences of exon and intron 23 of the mouse dystrophin gene were used. For intramuscular (i.m.) injections, 5 μg 2′-OMePSE23 with or without polymer was used in 40 μL saline for each tibialis anterior (TA) muscle. Mice were euthanized by CO_2 inhalation following 2 weeks treatment and muscles were snap-frozen in liquid nitrogen-cooled isopentane and stored at -80 ^{o}C.

Reverse transcription polymerase chain reaction (RT-PCR): Total RNA was extracted from tissue using TRIzol and 100 ng of RNA template was used for a 50 μL RT-PCR with the Stratascript One-Tube RT-PCR System (Stratagene, Santa Clara, CA). The primer sequences for the RT-PCR were Ex20Fo 5′-CAGAATTCTGCCAATTGCTGAG-3′ and Ex26Ro 5′- TTCTTCAGCTTGTGTCATCC-3′ for amplification of mRNA from exons 20 to 26. A total of 40 cycles was carried out for the RT-PCR. Bands with the expected size of the transcript with exon 23 deleted were extracted and sequenced. The intensity of the bands of PCR-amplified products obtained from the treated muscles was measured by the National Institutes of Health (NIH) ImageJ software 1.42, and the percentage of exon-skipping was calculated with the intensity of the 2 bands representing both unskipped and skipped exons as 100%.

Antibodies, immunohistochemistry, and Western blots: Sections of 6 μm were cut from the muscles and then stained with a primary rabbit polyclonal antibody P7 for the dystrophin protein and detected by secondary goat anti-rabbit Igs Alexa 594 (Invitrogen). The dystrophin-positive fibers were assessed by percentage of dystrophin-positive fibers to all fibers in one section observed using the Olympus BX51 fluorescent microscope (Olympus America Inc., Milville, NY, USA). Digital images were taken using the Olympus DP Controller and DP Manager software (Olympus America Inc., Milville, NY, USA), and the muscle fibers were defined as dystrophin-positive when more than two-third of the single fiber showed continuous staining.

Protein extraction and Western blot were done as described previously.[5,7] Membranes were probed with NCL-DYS1 monoclonal antibody against dystrophin rod domain (Vector Laboratories, Burlingame, CA). The bound primary antibody was detected with secondary HRP-conjugated goat anti-mouse IgG (Santa Cruz Biotechnology, Santa Cruz, CA) and the ECL™ Western Blotting Analysis System (Perkin-Elmer, Waltham, MA). The intensity of the bands with appropriate size were measured and compared with that from normal muscles of C57BL/6 mice with the NIH ImageJ software. a-Actin was detected by rabbit anti-actin antibody (Sigma, St. Louis, MO).

4.5. Statistical analysis

The data were analyzed for statistical significance using Student's *t*-test with a value of $p < 0.05$ being considered statistically significant. Data were expressed as mean ± SD.

Acknowledgment

The authors thank Mrs. Daisy M. Ridings and Mr. Chad J. Dickerson with the Electron Microscopy Core Laboratory for the negative staining and TEM electron micrographs, also thank Dr. David M Foureau and Dr. Fei Guo for their technical assistance in Flow Cytometry and analysis, and Dr. Anthony R. Blaeser for constructive proof reading. Furthermore, the authors gratefully acknowledge the financial support by the Carolinas Muscular Dystrophy Research Endowment at the Carolinas HealthCare Foundation and Carolinas Medical Center, Charlotte, NC.

The authors declare no conflicts of interest in relation to this paper.

References

1. E.P. Hoffman, R.H. Jr.Brown, L.M. Kunkel, *Cell,* 1987, **51**, 919-928.

2. M. Koenig, A.H.Beggs, M. Moyer, S. Scherpf, K. Heindrich, T. Bettecken, et al., *Am. J. Hum. Genet.,* 1989, **45**, 498-506.

3. V. Dubowitz, *Neuromuscul. Disord.,* 2005, **15**, 642-647.

4. K.R. Wagner, N. Lechtzin, D.P. Judge, *Biochim. Biophys. Acta,* 2007, **1772**, 229-237.

5. B. Wu, H.M. Moulton, P.L. Iversen, J. Jiang, J. Li, C.F. Spurney, et al., *Proc. Natl. Acad. Sci. USA,* 2008, **105**, 14814-14819.

6. H. Yin, H.M. Moulton, Y. Seow, C. Boyd, J. Boutilier, P. Iverson, M.J. Wood, *Hum. Mol. Genet.,* 2008, **17**, 3909-3918.

7. B. Wu, C. Cloer, M. Shaban, H. Moulton, P. Lu, Q. Lu, *Am. J. Pathol.,* 2012, **181**(2), 392-400.

8. N.M. Goemans, M. Tulinius, J.T. vanden Akker, B.E. Burm, P.F. Ekhart, N. Heuvelmans, et al., *N. Engl. J. Med.,* 2011, **364**, 1513-1522.

9. S. Cirak, V. Arechavala-Gomeza, M. Guglieri, L. Feng, S. Torelli, K. Anthony, et al., *Lancet,* 2011, **378**, 595-605.

10. J. Mendell, L,R. Rodino-Klapac, Z. Sahenk, K. Roush, L. Bird, L.P. Lowes, et al., *Ann. Neurol.,* 2013, **74**, 637-647.

11. K. Foster, H. Foster, J.G. Dickson, *Gene Ther.,* 2006, **13**, 1677-1685.

12. A. Aartsma-Rus, A.A. Janson, W.E. Kaman, M. Bremmer-Bout, G.J. van Ommen, J.T. den Dunnen, *et al*., *Am. J. Hum. Genet.,* 2004, **74**(1), 83-92.

13. C.L. Tanganyika-de Winter, H. Heemskerk, T.G. Karnaoukh, M. van Putten, S.J. de Kimpe, J. van Deutekom, A. Aartsma-Rus, *Mol. Ther. Nucl. Acids,* 2012, **1**, e43.

14. P. Järver, L. O'Donovan, M.J. Gait, *Nucleic Acid Ther.,* 2014, **24**(1), 37-47.

15. T. Koo, and M.J. Wood, *Hum. Gene Ther.,* 2013, **24**, 479-488.

16. F. Eckstein, *Antisense Nucleic Acid Drug Dev.,* 2000, **10**, 117-121.

17. J.C. van Deutekom, A.A. Janson, I.B. Ginjaar, et al., *N. Engl. J. Med.,* 2007, **357**, 2677-2686.

18. P.A. 't Hoen, C.G. van der Wees, A. Aartsma-Rus, R. Turk, A. Goyenvalle, O. Danos, et al., *Pharmacogenomics,* 2006, **7**, 281-297.

19. E. P. Hoffman, *N. Engl. J. Med.*, 2007, **357**, 2719-2722.

20. P. Rimessi, P. Sabatelli, M. Fabris, P. Braghetta, E. Bassi, P. Spitali, et al., *Mol. Ther.,* 2009, **17**(5),820-827.

21. S.R. Sirsi, R.C. Schray, X. Guan, N.M. Lykens, J.H. Williams, M.L. Erney, et al., *Hum. Gene Ther.,* 2008, **19**, 795-806.

22. J.H. Williams, S.R. Sirsi, D.R. Latta, G.J. Lutz, *Mol. Ther.,* 2006, **14**, 88-96.

23. C.L. Gebhart, S. Sriadibhatla, S. Vinogradov, P. Lemieux, V. Alakhov, A.V. Kabanov, *Bioconjug. Chem.,* 2002, **13**, 937-944.

24. M. Wang, B. Wu, P. Lu, C. Cloer, J.D. Tucker, Q. Lu, *Mol. Ther.,* 2013, **21**, 210-216.

25. M. Wang, B. Wu, P. Lu, J.D. Tucker, S. Milazi, S.N. Shah, Q. Lu, *Gene Ther.,* 2014, **21**, 52-59.

26. Y. Huang, Y. Rao, J. Chen, V.C. Yang, and W. Liang, *J. Biomed. Mater. Res. A*., 2011, **96**(3), 513-519.

27. A. Alshamsan, A. Haddadi, V. Incani, J. Samuel, A. Lavasanifar, H. Uludağ, *Mol. Pharm.,* 2009, **6**, 121-133.

28. K. Alexandridis, B. Lindman, Amphiphilic Block Copolymers Self-assembly and Application. Elsevier. 2000, ISBN: 978-0-444-82441-7.

29. X.B. Xiong, Z. Binkhathlan, O. Molavi, A. Lavasanifar, *Acta Biomaterialia,* 2012, **8**, 2017-2033.

30. M. Wang, B. Wu, J.D. Tucker, P. Lu, S.N. Shah, S. Wade, Q. Lu, *J. Nanomed. Nanotechnol.,* 2014, **5**, 228.

31. V. Prasad, S. Hashim, A. Mukhopadhyay, S.K. Basu, and R.P. Roy, *Antimicrob Agents Chemother*, 1999, **43** (11) 2689-2696.

32. M. Ruponen, S. Ronkko, P. Honkakoski, J. Pelkonen, M. Tammi, A. Urtti, *J. Biol. Chem.,* 2001, **276** (36), 33875-33880.

Captions

Scheme-1. Synthesis of T85-LPEI copolymers (Z polymers).

Table 1. Characteristics of T85-LPEI copolymers (Z polymers)

Figure 1. Electrophoretic mobility of polymer/oligonucleotide complexes at four weight ratio of Rw = 0.2 , 0.5 , 1 and 2 (from left to right for each polymer). 1 µg oligonucleotide in a total of 24 µL medium was used. The 1st lane on the left is loaded with 1 µg oligonucleotide only.

Figure 2. Biophysical properties of polymer-oligonucleotide complex (Rw = 5). A) Particle sizes analyzed by DLS, Inserted is the distribution of size; B) Negative staining TEM images (scale bar 200 nm).

Figure 3. Stability of complexes [Polymer/oligonucleotide = 2/1(Rw = 2)] to serum or heparin. A) In the presence of serum. 4 lanes for each polymer with FBS concentration of 0, 10, 25, 50% from left to right; The middle bands between the oligonucleotide (bottom bands) and wells (top bands) are non-specific binding of EB to serum components. B) In the presence of sodium heparin (0, 10, 25, 50 µg/mL) from left to right.

Figure 4. The cytotoxicity of the Z polymers in C2C12E50 cell lines with MTS-based cell viability assay. The polymer dosages are 4, 10, 20 µg/mL from left to right for each sample. Cells were seeded in 96 well plates at an initial density of 1 x 10^4 cells/well in 0.2 ml growth media. The results are presented as the mean ± SD in triplicate (Student's t-test, $*p \leq 0.05$ compared with untreated cell as a control).

Figure 5. Dose-dependent GFP expression of polymer Z7 formulated 2′-OMePS: 2 µg 2′-OMePS with polymers in 0.5 mL 10% FBS-DMEM incubated under 37°C, 10% CO_2 environment. The images were taken 48 hrs after transfection.

Figure 6. A) Representative fluorescence images of 2′-OMePSE50 -induced exon-skipping in C2C12E50 cell line. The images were taken 48hr after treatment. Original magnification, x100. B) Transfection efficiency of 2′-OMePSE50 formulated with polymers (Student's t-test, $*p \leq 0.05$ compared with 2′-OMePS only). C) Cell viability (Student's t-test, $*p \leq 0.05$ compared with untreated cells as a control). 2 µg of 2′-OMePSE50 were

formulated with Zs (5,10 μg), and PEI-25k (2, 5 μg), LF-2k (4 μg) formulated as controls in 0.5 mL 10% FBS-DMEM medium, respectively. The results are presented as the mean ± SD in triplicate.

Figure 7. Intracellular interaction of FITC-labeled-Z9 formulated with Cy3-labeled-oligonucleotide (Cy3-Oligo) in C2C12 fibroblast cell line (10 μg polymer in 0.5 mL 10% FBS-DMEM with Cy3-Oligo 2 μg). (A-A′) Nuclei were stained with Hoechst 33258 (blue fluorescence); (B-B′) Red fluorescent signal from labeled Cy3-Oligo; (C-C′) Green fluorescence arising from FITC-labeled-polymer; (D-D′) Merged image (A+B+C) demonstrating localization of the polymer relative to AO signal. Yellow fluorescence on the merged image (D) indicates where FITC-polymer and Cy3-Oligo are collocated, contrasted with red signal from oligonucleotide dissociated from the initial polymer-AO complex. 40 x magnification.

Figure 8. Dystrophin exon-skipping and protein expression following i.m. administration of 2′-OMePS E23 without and with polymers in TA muscle of *mdx* mice (aged 4-5 weeks) after 2 week treatment. Muscles were treated with 2′-OMePSE23 (5 μg) and polymer (10 μg) in 40 μL saline. 2′-OMePS E23 (5 μg) only was used as control: ***A)*** Restoration of dystrophin in TA muscle was detected by immunohistochemistry with rabbit polyclonal antibody P7 against dystrophin. Blue nuclear staining with DAPI (4,6-diamidino-2-phenylindole). Original magnification, x100. ***B)*** The percentage of dystrophin-positive fibers in a single cross-section induced by 2′-OMePS E23 with/without polymer formulation (average ± SD, n = 5, Student's t-test, $*p \leq 0.05$ compared with 5 μg 2′-OMePSE23). ***C)*** Detection of exon 23 skipping by RT-PCR. Total RNA (100 ng) of from each sample was used for amplification of dystrophin mRNA from exon 20 to exon 26. The upper bands (indicated by E22+E23+E24) correspond to the normal mRNA and the lower bands (indicated by E22+E24) correspond to the mRNA with exon E23 skipped. ***D)*** Western blot demonstrates the expression of dystrophin protein from treated *mdx* mice compared with C57BL/6 and untreated *mdx* mice. Dys: dystrophin detected with a monoclonal antibody ManDys 1. a-Actin was used as the loading control.